IMPLEMENTATION RESULTS OF μ-SYNTHESIS CONTROL FOR AN ENERGY STORAGE FLYWHEEL TEST RIG

Ulrich Schönhoff[1], Jihao Luo[2], Guoxin Li[3], Edgar Hilton[3], Rainer Nordmann[1], Paul Allaire[3]

[1]Darmstadt University of Technology, Department of Mechanical Engineering, Darmstadt, Germany, Schoenhoff@mum.tu-darmstadt.de, Nordmann@mum.tu-darmstadt.de, resp.

[2]American Flywheel Systems Inc., Charlottesville, Va, USA, Jihao.Luo@amfwheel.com

[3]University of Virginia, Department of Mechanical and Aerospace Engineering, Charlottesville, Va, USA, gl2n@virginia.edu, efh4v@virginia.edu, pea@virginia.edu, resp.

ABSTRACT

In this paper μ-synthesis is applied to a flexible and gyroscopic AMB system. A design methodology is presented which covers the practical issues of robust control like the selection of weighting functions, modelling of uncertainties and controller reduction. The modelling of the system is based on a analytical model adjusted to measured frequency responses. Special attention is paid to substructure modes. The focus of this paper is the experimental evaluation of the performance. Sine sweeps were performed at rotational speed and good agreement of the measured performance with the predicted robust performance is reached. The test rig finally was spun up past the first flexible critical speed.

INTRODUCTION

Robust control design methods, particularly the μ-synthesis, have great potential for AMB applications, but have not found their way to application yet. Implementation results are only reported by Fujita *et al*. (1992), Nonami and Ito (1994), and Fittro and Knospe (1998) so far. Fujita considers the non-rotating case only. Nonami's design is based on a rigid-body model. Only Fittro gives experimental results in frequency domain. A systematic experimental evaluation of the robust performance was not performed yet. Related work on non-AMB applications giving experimental results are Steinbuch *et al*. (1998) and Van den Braembussche (1998).

The AMB controls test rig at the University of Virginia is designed to reflect the properties of energy storage flywheels, namely the gyroscopics and the structural flexibilities of the rotor and the frame, and to serve as a platform for controller design investigations. The flexible rotor is equipped with a overhung gyroscopic disc (Fig. 1) and aligned vertically. The substructure is designed to be flexible as well, to simulate a satellite platform.

In order to operate the rotor in a range up to 12000 rpm, a μ-synthesis controller was designed and the experimental results are presented in this paper. It is based on the design procedure developed in Schönhoff *et al*. (2000). This procedure unifies the required design steps for systems with structural flexibilities and aims a easy transferability to different applications.

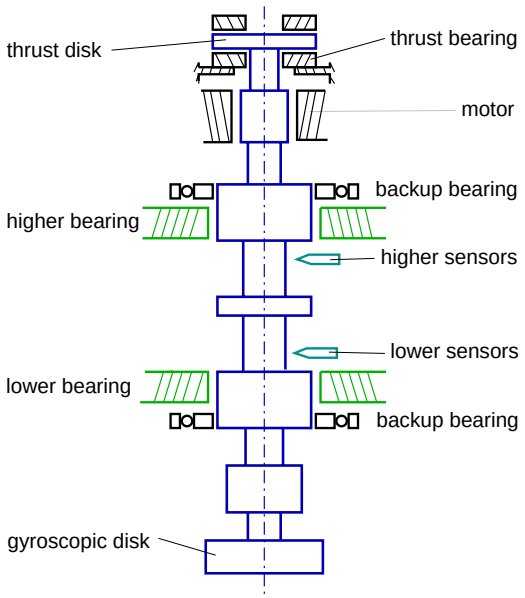

FIGURE 1: Schematic of the rotor

MODELLING

The model of the plant was first derived analytically and then fine tuned based on frequency response measurements of the plant. Since the plant itself is unstable, the system was stabilized by an initial PID controller and the closed loop response was measured. The computa-

tion of the plant model from the closed loop response is described in the section “implementation results”.

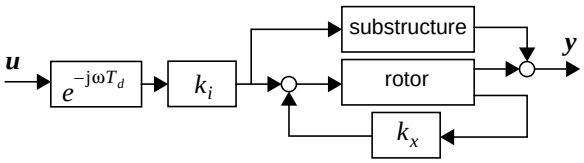

FIGURE 2: Block diagram of the plant model with black-box model of the substructure

The plant model for the controller design covers the structural dynamics of the rotor and of the substructure, the magnetic bearings, the amplifiers and the control computer (Fig. 2). The structural dynamics of the rotor was first modelled by finite element modelling and then fine tuned based on experimental results. The rotor model includes 4 rigid-body and 6 flexible modes. A model of the gyroscopic effects was also obtained from finite element analysis and validated at rotational speed. Fig. 4 shows the Campbell-diagram of the unrestrained rotor.

Since the substructure had a significant impact on the system stability and performance, also a substructure model was included. It was constructed solely based on experimental data by curve-fitting of the measured frequency responses. 12 modes have been taken into consideration. Since controller order reduction methods are utilized, no attempt was made to reduce the plant model in advance of the controller design.

The magnetic bearing is described by a linearized displacement-force and current-force relation $f = k_x x + k_i i$ (Rockwell, 1996). These parameters were tuned to match the measured frequency responses of the plant. Additionally a negative stiffness of the motor had to be taken into account.

No specific dynamic model for amplifier, the inductance and further electronic components was set up. The phase lag of these components including the phase lag of the zero-order hold of the D/A-converter and the computation time of the digital control computer were also determined from the measured frequency responses and modelled by a total time delay of 0.625 ms. The time delay was approximated by a 2nd order Pade allpass filter per input. The final order of the plant model is 52.

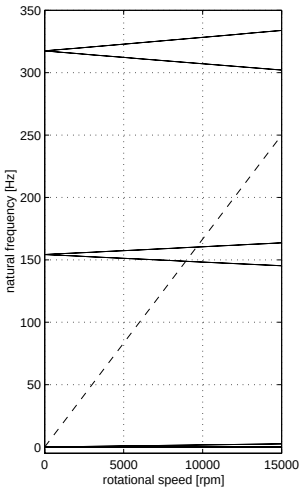

FIGURE 3: Campbell-diagram of the unrestrained rotor

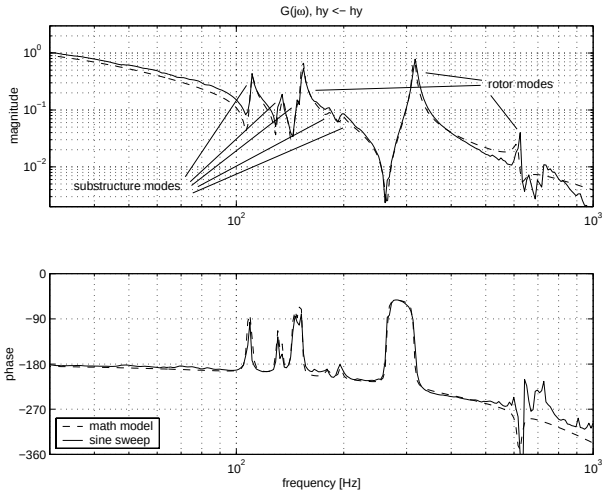

FIGURE 4: Exemplary channel $\boldsymbol{G}_{(\mathrm{hy,hy})}$ (from higher bearing *y*-direction to higher sensor *y*-direction) of the 4×4 plant model at 0 rpm

CONTROLLER DESIGN

Performance specification

Specifying the performance requirements for H_∞-minimization means bounding the transfer functions of the closed loop. This is a non trivial task, neither in terms of H_2-performance nor in terms of reasonable time response of the closed loop. To formulate the specifications, a proper insight in the transfer functions of the closed loop is required.

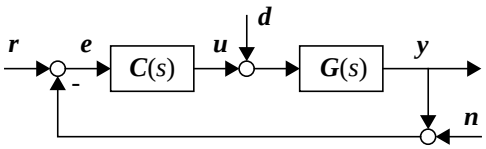

Figure 5: Closed control loop

Fig. 5 depicts the control loop, where ***y*** are the displacement measurements, ***r*** the reference commands, ***e*** the displacement errors, ***u*** the current command to the amplifiers, ***d*** a assumed disturbance and ***n*** the sensor noise. Each of these variables consists of four components for each of the two axes per bearing. The transfer function matrix

$$\begin{bmatrix} \boldsymbol{y}(s) \\ \boldsymbol{e}(s) \\ \boldsymbol{u}(s) \end{bmatrix} = \begin{bmatrix} \boldsymbol{T}(s) & \boldsymbol{S}(s)\boldsymbol{G}(s) & -\boldsymbol{T}(s) \\ \boldsymbol{S}(s) & -\boldsymbol{S}(s)\boldsymbol{G}(s) & -\boldsymbol{S}(s) \\ \boldsymbol{C}(s)\boldsymbol{S}(s) & -\boldsymbol{T}_i(s) & -\boldsymbol{C}(s)\boldsymbol{S}(s) \end{bmatrix} \begin{bmatrix} \boldsymbol{r}(s) \\ \boldsymbol{d}(s) \\ \boldsymbol{n}(s) \end{bmatrix} \quad (1)$$

gives the relation between the inputs and outputs of the closed loop.

The minimization of the transfer function $\boldsymbol{S}(\mathrm{j}\omega)\boldsymbol{G}(\mathrm{j}\omega)$ is the main objective. It can be viewed as the “compliance” of the magnetic bearing. A constant bound is put on this function in order to achieve a low quasi-static compliance

and to enforce proper damping of the first flexible mode of the rotor (Fig. 7). Levelling off the bound at low frequencies yields integral action of the controller.
The actuator effort is described by $\boldsymbol{C}(j\omega)\boldsymbol{S}(j\omega)$. A bound on this transfer function avoids actuator saturation. $\boldsymbol{C}(j\omega)\boldsymbol{S}(j\omega)$ has further to be limited for two reasons: First $(\boldsymbol{C}(j\omega)\boldsymbol{S}(j\omega))^{-1}$ determines the robustness to additive uncertainties of the plant and is desired to be high. Second it determines the shape of $\boldsymbol{C}(j\omega)$ at high frequencies, because $\lim_{\omega\to\infty} \boldsymbol{S}(j\omega) = 1$. A low pass characteristic of $\boldsymbol{C}(j\omega)$ rejects sensor noise and is advantageous for controller order reduction and discrete time implementation. A second order low pass bound was chosen (Fig. 7).
Even though bounding of $\boldsymbol{S}(j\omega)\boldsymbol{G}(j\omega)$ and $\boldsymbol{C}(j\omega)\boldsymbol{S}(j\omega)$ is sufficient to set up the optimization problem, limiting the sensitivity function $\boldsymbol{S}(j\omega)$ and the inverse sensitivity function $\boldsymbol{T}(j\omega)$ additionally is very useful to obtain reasonable controllers. A sensitivity function $\boldsymbol{S}(j\omega) > 1$ indicates that the controller is amplifying the disturbances entering the system. For lightly damped flexible structures, putting a strict bound on $\boldsymbol{C}(j\omega)\boldsymbol{S}(j\omega)$ will cause the resonances of $\boldsymbol{G}(j\omega)$ to appear in $\boldsymbol{T}(j\omega)$ with high peaks. This is undesired in all three meanings of $\boldsymbol{T}(j\omega)$ resp. $\boldsymbol{T}_i(j\omega)$: the reference action, the actuator response to disturbance and the transmission of sensor noise to the controlled variable. For details on the weighting functions see Schönhoff *et al*. (2000) and Van den Braembussche (1998).
To realize this SG-CS-S-T weighting scheme, the inputs $\boldsymbol{w}$ and $\boldsymbol{d}$ and the outputs $\boldsymbol{y}$, $\boldsymbol{e}$ and $\boldsymbol{u}$ were chosen and augmented with the corresponding weighting functions $\boldsymbol{W}_{r..u}$:

$$F_l(\boldsymbol{P},\boldsymbol{C}) = \begin{bmatrix} \boldsymbol{W}_y\boldsymbol{T}\boldsymbol{W}_r & \boldsymbol{W}_y\boldsymbol{S}\boldsymbol{G}\boldsymbol{W}_d \\ \boldsymbol{W}_e\boldsymbol{S}\boldsymbol{W}_r & -\boldsymbol{W}_e\boldsymbol{S}\boldsymbol{G}\boldsymbol{W}_d \\ \boldsymbol{W}_u\boldsymbol{C}\boldsymbol{S}\boldsymbol{W}_r & -\boldsymbol{W}_u\boldsymbol{T}_i\boldsymbol{W}_d \end{bmatrix}. \qquad (2)$$

The weighting functions were designed to realize the desired bounds, e.g. $\bar{\sigma}(\boldsymbol{C}\boldsymbol{S}) < \bar{\sigma}(\boldsymbol{W}_u\boldsymbol{W}_r)^{-1}$. All weights are chosen to have diagonal structure and equal diagonal elements.

Uncertainty modelling

Robustness to parameter variations of the plant and to modelling errors is a requirement for practical control. Here the controller has to cope with

- uncertainty in the modelling of the flexible structure,
- variation of the natural frequencies due to the gyroscopic effect and
- changes in the magnetic bearing parameters.

Modelling errors in lightly damped flexible structures are typically due to small mismatches in the resonances. Since even small mismatches can cause large additive respectively multiplicative errors, they are modelled as parametric uncertainties in natural frequencies (Balas, Young, 1995). Assume that the system matrix $\boldsymbol{A}$ of the rotor and substructure subsystem of the plant model is transformed by $\boldsymbol{T}$ to a real modal representation $\tilde{\boldsymbol{A}} = \boldsymbol{T}\boldsymbol{A}\boldsymbol{T}^{-1}$, where

$$\tilde{\boldsymbol{A}}_i = \begin{bmatrix} 0 & 1 \\ -(\omega_i(1+\delta_i))^2 & -2\xi_i\omega_i(1+\delta_i) \end{bmatrix} \qquad (3)$$

is the 2×2 block for the ith mode on the diagonal of $\tilde{\boldsymbol{A}}$ and ω_i is the natural frequency of this mode with the relative uncertainty δ_i. The modal damping ξ_i is assumed to be constant, since it turned out to have no relevant influence on the controller design. Linearizing the term $(\omega_i(1+\delta_i))^2$ to $\omega_i^2 + 2\omega_i^2\delta_i$, which is valid for the small uncertainties assumed, $\boldsymbol{A}_i$ can be rewritten as

$$\tilde{\boldsymbol{A}}_i \approx \begin{bmatrix} 0 & 1 \\ -\omega_i^2 & -2\xi_i\omega_i \end{bmatrix} + \begin{bmatrix} 0 \\ 1 \end{bmatrix} \delta_i \begin{bmatrix} -2\omega_i^2 & -2\xi_i\omega_i \end{bmatrix} \qquad (4)$$

and the uncertainty can be represented in a LFT a single real uncertainty δ_i. Here an uncertainty of ±3 % in all 18 flexible modes is considered.
The uncertainty in natural frequencies already covers the variation of the natural frequencies due to the gyroscopic effects. But more structured in the sense of μ-synthesis is the treatment of the gyroscopic effects as an uncertainty itself. Therefor the system matrix $\boldsymbol{A}(\Omega)$ of the plant, dependent on the rotational speed Ω, is considered as nominal matrix plus a gyroscopic term linear in Ω: $\boldsymbol{A}(\Omega) = \boldsymbol{A}_0 + \boldsymbol{A}_G\Omega$. This uncertainty can be represented in a LFT with the number of repeated uncertainty as a the rank of $\boldsymbol{A}_G$, e.g. by singular value decomposition of $\boldsymbol{A}_G$ (Balas *et al*., 1995, 4-20). The rank of $\boldsymbol{A}_G$ is equal to the number of flexible modes of the rotor plus the number of tilt rigid-body modes, here 6 + 2 = 8.
The robustness to variations in the magnetic bearing parameters is a further crucial issue. The parameters depend significantly on the operating point and vary with displacement and bearing coil currents. Since the complex weighting scheme, used in this design, already guarantees robust stability to large additive uncertainties by bounding $\boldsymbol{C}\boldsymbol{S}$ and to large multiplicative uncertainties by bounding $\boldsymbol{T}$, the parameter variations were not taken into account explicitly as suggested in Namerikawa, Fujita (1998). Theoretical and experimental analysis of the control loop have confirmed the robustness.

μ-Synthesis

Two different designs were performed: The first design considers uncertainties in natural frequencies only. It was designed for an operation point of 10000 rpm in order to optimize the design for passing the critical speed. The augmented plant has 72 states, a 12×8 unstructured performance block and 18 real scalar uncertainties in the natural frequencies.
The second design additionally includes the gyroscopics

as uncertainty. The augmented plant increases by 8 additional real repeated uncertainties.

The controller synthesis was carried out using the D-K-Iteration (Balas *et al.*, 1995). To perform the D-K-Iteration, several measures had to be taken to avoid numerical problems. Two other μ-synthesis approaches, the (D,G)-K- and the μ-K iteration were investigated to take advantage of the real and repeated structure of the uncertainties, but did not converge in this case due to numerical problems. Details on the numerical issues are given in Schönhoff *et al.* (2000).

The first controller reached a μ-value of 1.06. μ-analysis for different rotational speeds was performed to determine the stability and performance of this controller vs. rotational speed (Fig. 6). The controller turned out to be stabilizing up to 25000 rpm. The μ-values of the second controller treating the gyroscopics as an additional uncertainty are given in Table 1 dependent on the considered range of operation speeds. The order of the final controllers were in both cases larger than 100.

speed range [rpm]	$\sup(\mu_\Delta(F_l(\boldsymbol{P},\boldsymbol{C})))$
10000,fix	1.06
0 .. 14000	1.12
0 .. 30000	1.44
0 .. 60000	2.02

TABLE 1: μ vs. considered speed range for gyroscopic treated as

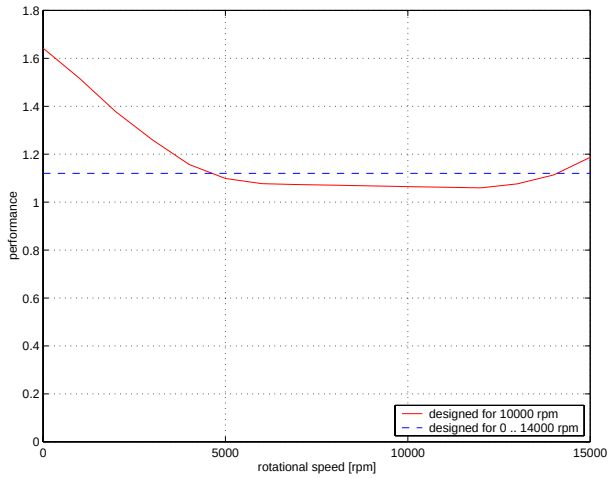

FIGURE 6: Robust performance vs. rot speed for the first design

Controller order reduction

In order to achieve high accuracy, the pant was modelled without respect to the model order. But as well as accurate modelling is necessary for reliable application, a low order of the controller is a prerequisite for economic realisation. Because the controller is of the order of the augmented plant plus the order of the D-scales added by the D-K-iteration, this leads to a contradiction that can only be solved by controller reduction methods.

In order to reach the maximum degree of reduction, it is straight forward to address the preservation of robust performance

$$\min_{\hat{C}} \sup_{\omega}(\mu_\Delta(F_l(\boldsymbol{P},\boldsymbol{C}))-\mu_\Delta(F_l(\boldsymbol{P},\hat{\boldsymbol{C}}))) \qquad (5)$$

directly, where $\boldsymbol{C}$ is the original controller and $\hat{\boldsymbol{C}}$ is the reduced one. By replacing μ with its upper bound and using the D-scalings as in D-K-iteration, $\mu_\Delta(F_l(\boldsymbol{P},\boldsymbol{C}))$ becomes $\bar{\sigma}(\boldsymbol{D}_l F_l(\boldsymbol{P},\boldsymbol{C})\boldsymbol{D}_r^{-1})$ and the minimization problem can be formulated in terms of rational transfer functions (Rivera, Morari, 1992):

$$\min_{\hat{C}} \left\| \boldsymbol{D}_l F_l(\boldsymbol{P},\boldsymbol{C})\boldsymbol{D}_r^{-1} - \boldsymbol{D}_l F_l(\boldsymbol{P},\hat{\boldsymbol{C}})\boldsymbol{D}_r^{-1} \right\|_\infty . \qquad (6)$$

This can directly be tackled by the frequency weighted balanced reduction in closed loop configuration (Wortelboer *et. al.*, 1999). A reduction from an order higher than 100 to 44 is reached here without significant loss in performance (1%).

IMPLEMENTATION RESULTS

In this section experimental results for the first controller design considering uncertainties in the natural frequencies only are presented. The controller was implemented on a PC using the *Realtime Linux* based *Real Time Controls Laboratory* (RTiC-Lab) software (Hilton *et al.*, 2000). It was executed at a sampling rate of 8 kHz.

The test rig was successfully spun up to 12000 rpm and three critical speeds, two rigid-body and one flexible were passed. The flexible critical is at about 9500 rpm. It turned out that the controller provides high damping for all three modes and therefore the vibration is well within the acceptable range (Fig. 9). The maximum of the actuator effort is approximately 0.6 A, where the actuators become saturated at 2 A.

In order to evaluate the performance experimentally, sine sweeps were performed at two rotational speeds, 0 and at 6000 rpm. A sinusoidal excitation $\boldsymbol{d}$ was superposed to the control output and the displacement $\boldsymbol{y}$ was measured. Fig. 7 shows the maximum singular value $\bar{\sigma}(\boldsymbol{SG})$ computed from the measured frequency response matrix $\boldsymbol{SG}$ at 6000 rpm. It is compared to the nominal transfer function from the model. Additionally the bounds given by the weighting functions are shown. The remaining frequency responses of the closed loop $\boldsymbol{CS}$, $\boldsymbol{S}$, $\boldsymbol{T}$ and $\boldsymbol{T}_i$ according to (1) were computed from the measured frequency response $\boldsymbol{SG}$ and the open-loop measured frequency response of the controller $\boldsymbol{C}$ according to the relations $\boldsymbol{T} = (\boldsymbol{SG})\boldsymbol{C}$, $\boldsymbol{T}_i = \boldsymbol{C}(\boldsymbol{SG})$, $\boldsymbol{S} = \boldsymbol{I}-\boldsymbol{T}$, $(\boldsymbol{CS}) = \boldsymbol{CS}$ and $\boldsymbol{G} = \boldsymbol{S}^{-1}(\boldsymbol{SG})$. They are also depicted in Fig. 7.

Since the comparison with the nominal model does not answer the question, if the predicted robust performance is reached, the maximum singular value of the total performance is processed from all measured and computed frequency responses multiplied with the weighting func-

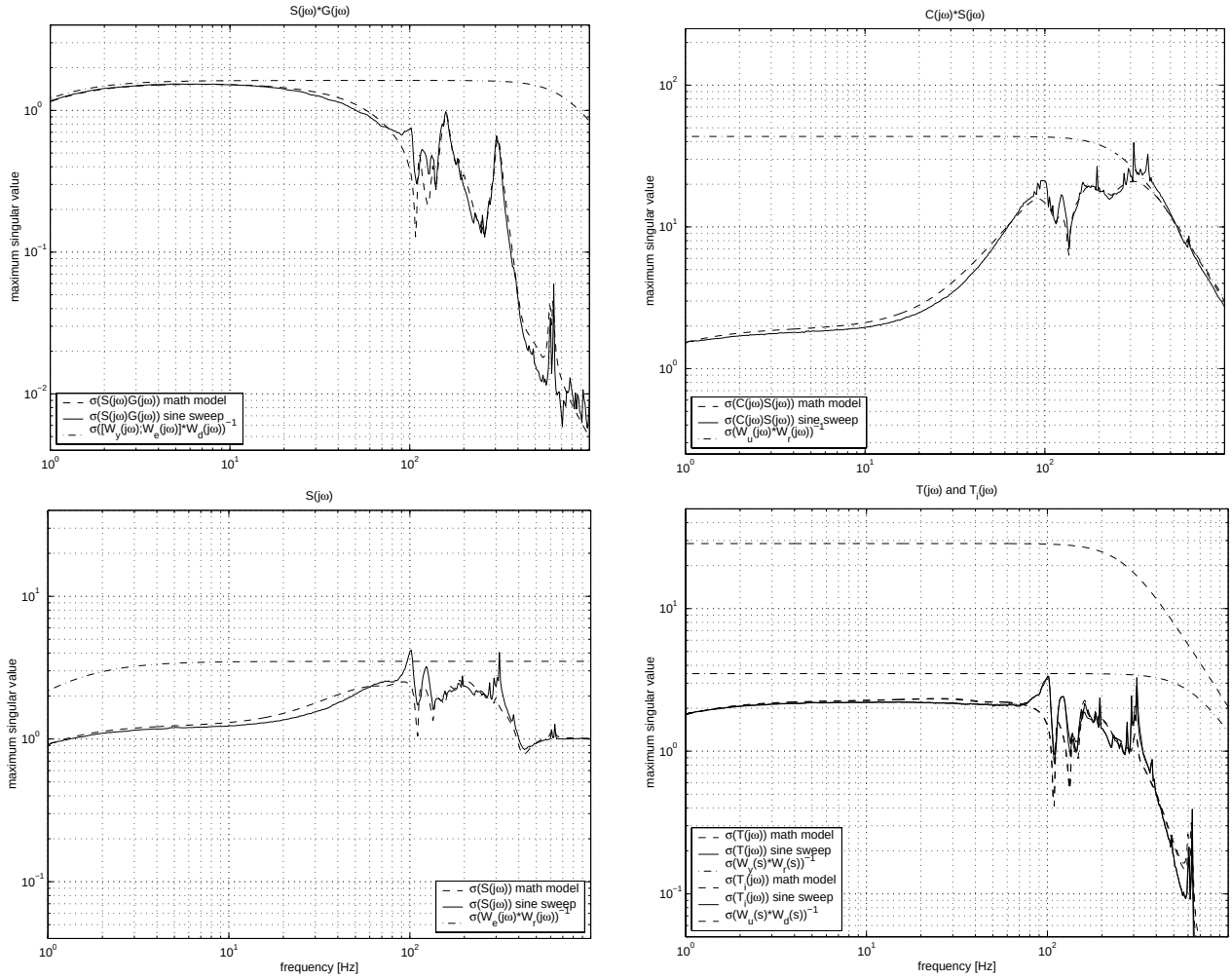

FIGURE 7: Measured and nominal frequency responses of the closed loop for the first μ-synthesis controller and their bounds at 6000 rpm

tions according to (2). This is shown in Fig. 8 for the measurements at 0 and 6000 rpm and compared to the expected robust performance obtained by μ-analysis at the particular operation points. Note that both points of oper-

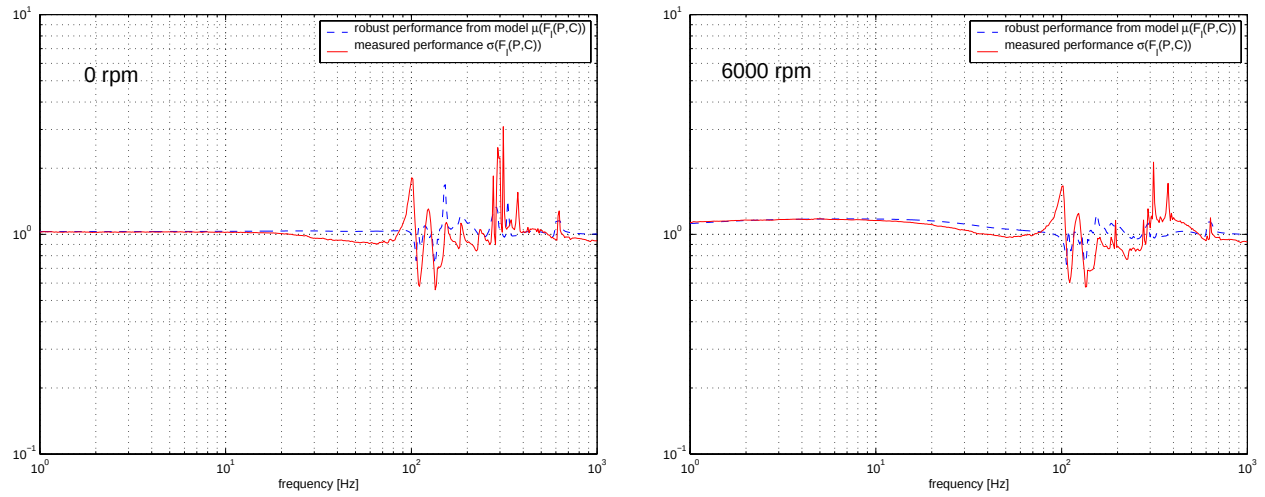

FIGURE 8: Measured performance (maximum singular values of the augmented plant) and robust performance μ of the closed loop for the first μ-synthesis controller at 0 and 6000 rpm

ation, 0 and 6000 rpm are outside of the design point at 10000 rpm. Peaks occurring in $\boldsymbol{S}$ and $\boldsymbol{CS}$ and $\bar{\sigma}(F_l(\boldsymbol{P},\boldsymbol{C}))$ can partly be explained by numerical singularities in processing the measured data. The remainder is due to unmodelled substructure modes. The performance decrease at low frequencies for the measurement at 6000 rpm is caused by the negative stiffness of the rotor.

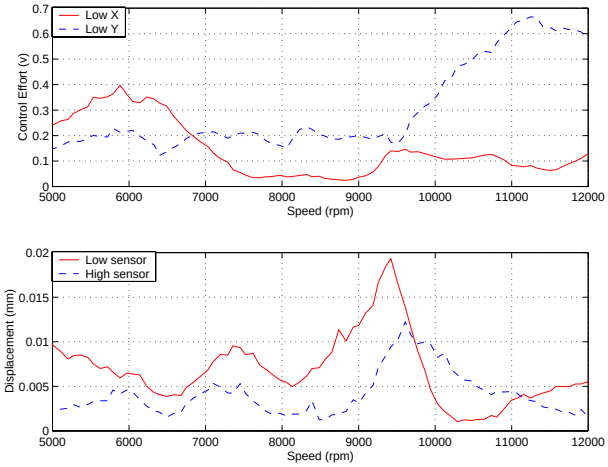

FIGURE 9: Run down from 12000 rpm

Since the robustness to changes in the magnetic bearing parameters is crucial issue, the performance of the closed loop using was analysed for different bias currents. No significant performance degradation could be identified in a range from 0.75 A to 2.5 A, where 2 A is the nominal bias current.

CONCLUSIONS

In this paper, we developed μ-synthesis controller for a flexible AMB system with severe gyroscopic effects and substructure modes. The utilized design methodology overcame the practical issues involved in robust controller design. In particular modelling errors were considered in terms of uncertainties in the natural frequencies and the gyroscopic effects were treated as uncertainty as well. Using this controller, the test rig easily passed first flexible critical speed. Sine sweeps showed a good agreement of the measured performance and the predicted robust performance.

ACKNOWLEDGEMENTS

We would like to thank the German Academic Exchange Service DAAD for funding this work. Furthermore, we wish to acknowledge the NASA, Goddard Space Flight Center and American Flywheel Systems for supporting this research as an element of a Small Business Innovative Research (SBIR) project. We also thank Pepijn Wortelboer, who made the Wor-Toolbox for controller reduction available.

REFERENCES

Balas, G.J.; Doyle, J.C.; Glover, K; Packard, A.K; Scmith, R. (1995): μ-*Analysis and Synthesis Toolbox.* MUSYN Inc., Mineapolis, MN and The Mathworks, Inc., MA.

Balas, G.J.; Young, P.M. (1995): Control design for variations in structural natural frequencies. *J. of Guidance, Control and Dynamics* **18**(2), 325-332.

Fittro, R.L.; Knospe, C.R. (1998): μ-synthesis control design applied to a high speed machining spindle with active magnetic bearings. *6th Int. Symp. on Magnetic Bearings*, Cambridge, MA, USA, 449-458

Fujita, M.; Matsumura, F.; Namerikawa, T. (1992): μ-analysis and synthesis of a flexible beam suspension system. *2nd Int. Symp. on Magnetic Bearings*, Alexandria, Va, USA, 495-504.

Hilton, E.F., Humphrey, M.; Stankovic, J.; Allaire, P. (2000): Design of an open source, hard real time, controls implementation platform for active magnetic bearings. *7th Int. Symp. on Magnetic Bearings*, Zürich, Switzerland.

Namerikawa, T.; Fujita, M. (1998): Uncertainty structure and μ-design of a magnetic suspension system. *6th Int. Symp. on Magnetic Bearings*, Cambridge, MA, USA, 439-448.

Nonami, K.; Ito, T. (1994): μ-synthesis of flexible rotor of magnetic bearing system. *4th Int. Symp. on Magnetic Bearings*, Zürich, Switzerland, 73-78

Rivera, D.E.; Morari, M. (1992): Plant and controller reduction problems for closed-loop performance. *IEEE Trans. on Automatic Control* **37**(3), 398-404.

Rockwell, R.D.; Allaire, P.E.; Heinrich, J.C.; Fosage, G.K. (1996): Magnetic field modelling of magnetic bearings including rotor motion effect and eddy currents. *5th Int. Symp. on Magnetic Bearings*, Kanzawa, Japan, 241-246.

Schönhoff, U.; Klein, A.; Nordmann, R. (2000): Attitude Control of the Airborne Telescope SOFIA: μ-Synthesis for a Large Flexible Structure. Submitted to the *39th IEEE Conference on Decision and Control, CDC 2000*, Sydney, Australia, December 2000.

Steinbuch, M.; van Groos, P.J.M.; Schostra, G.; Wortelboer, P.M.R.; Bosgra, O.H. (1998): μ-Synthesis for a Compact Disc Player. *Int. J. of Robust and Nonlinear Control* **8**, 169- 189.

Van Den Braembussche, P. (1998): *Robust motion control of high-performance machine tools with linear motors*. Ph.D. Thesis, Katholieke Universiteit Leuven, Leuven, Belgium.

Wortelboer, P.M.R.; Steinbuch, M.; Bosgra, O.H. (1999): Iterative model and controller reduction using closed-loop balancing, with an application to a compact disc mechanism. *Int. J. of Robust and Nonlinear Control* **9**(3), 123-142.